Influence of the Ester Directing-Group on the

Inhibition of Defect Formation in Polythiophenes

with Direct Arylation Polymerization (DArP)

Robert M. Pankow^a, Liwei Ye^a, Barry C. Thompson^a*

^aDepartment of Chemistry and Loker Hydrocarbon Research Institute, University of Southern California, Los Angeles, California 90089-1661.

ABSTRACT. Direct arylation polymerization (DArP) has allowed for the facile preparation of a variety of conjugated polymer architectures. Since DArP proceeds through a C-H activation pathway, the selectivity of only the desired C-H bond for certain monomers has remained a challenge. Low selectivity for the desired C-H bond can lead to the introduction of various structural defects. The development of conditions through the use of additives, screening and design of phosphine ligands, as well as pre-catalysts has provided condition sets that work for some monomers to afford the desired polymers with a minimization of defects. In addition to modifying the conditions, another handle for tuning the site selectivity for C-H activation is through the introduction of a directing group, such as an ester. Ester functionalized conjugated polymers have gone through a renaissance of sorts where the inclusion of this functionality on thiophene based monomers has garnered increased attention. To understand how this functionality can be exploited as a directing-group for DArP, we study the formation of defects for poly(3-hexylesterthiophene-2,5-diyl) (P3HET) and select structural analogs. We develop optimized

conditions that allow for the synthesis of this polymer with improved molecular weight (M_n) (up to 15.9 versus 11.7 kDa) and regioregularity (up to >99% versus 96%) in a shorter polymerization time (16 versus 48 hours). Based on extensive defect analysis using ¹H-NMR spectroscopy we rationally design a monomer for the synthesis of the donor-acceptor polymer poly(2-Hexyldecyl [2,2'-bithiophene]-4-carboxylate -5,5'-diyl) (P3HDET-T) with good M_n (26.2 kDa) and regioregularity (>99%). This study shows how the inclusion of ester directing groups and the formulation of pathways for defect formation can enable the rational design of monomers yielding conjugated polymers with improved M_n and rr.

Introduction.

Conjugated polymers are designed for incorporation into a vast array of applications, ranging from organic electronics to biological devices.¹⁻⁴ In particular, ester-functionalized polythiophene conjugated polymers have garnered recent attention due to their facile synthesis and desirable electronic properties. Such polymers have been studied in applications, such as organic photovoltaic devices (OPV) and organic field-effect transistors (OFET).⁵⁻⁹ It has been shown that high regioregularity (rr) is important for obtaining a polymer with desirable electronic properties, and that regiorandom ester-functionalized polythiophenes suffer from diminished device performance.^{5,8,10} Of the numerous ester-functionalized polythiophenes, one of the most well studied and characterized is poly(3-hexylesterthiophene-2,5-diyl) (P3HET), which has been reported using a variety of polymerization methods (see Figure 1A). These methods include Stille-Migita (P3HET-Stille),¹¹ direct arylation polymerization (P3HET-DArP),¹¹ oxidative direct arylation (P3HET-Oxi-DArP),¹² and Suzuki-Miyaura catalyst transfer polymerization (P3HET-SCTP).¹³ Also detailed in Figure 1A, are the monomer structures, corresponding polymerization

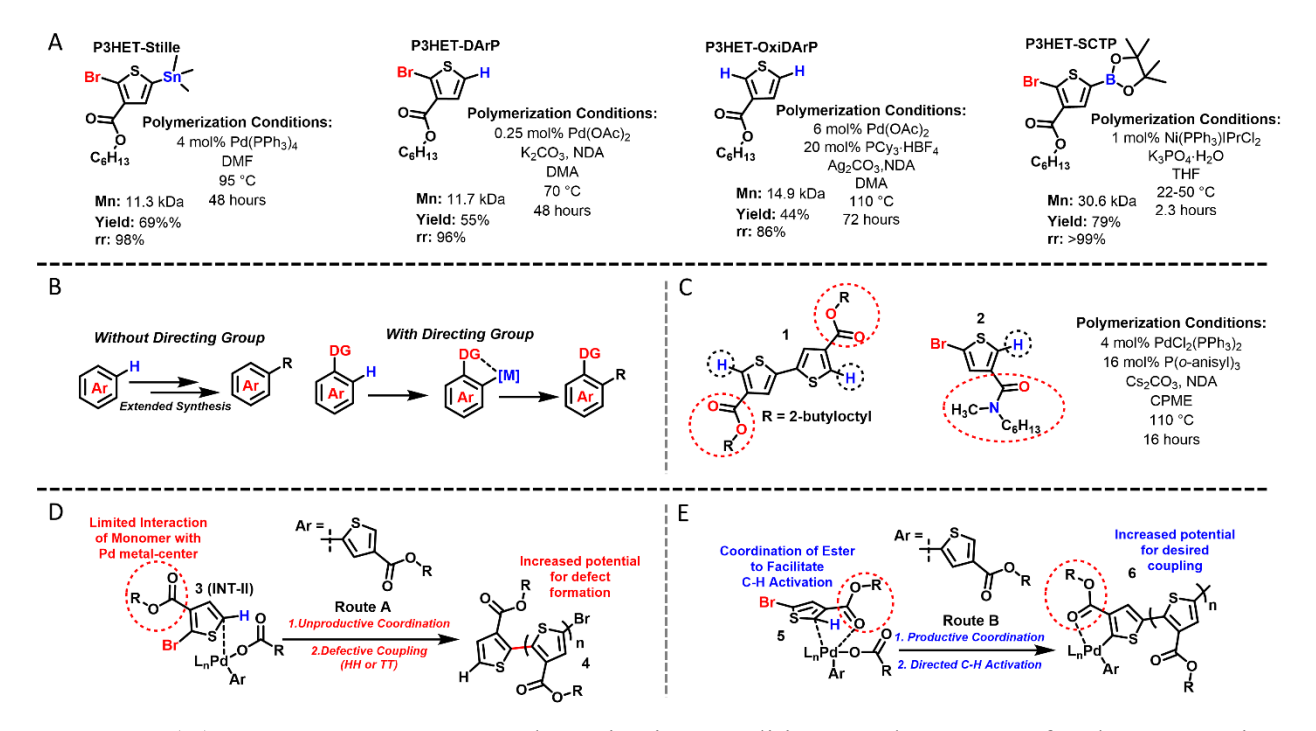


Figure 1. (A) Monomer structures, polymerization conditions, and outcomes for the preparation of P3HET via Stille, DArP, Oxi-DArP, and SCTP (DMF is dimethylformamide, DMA is dimethylacetamide, NDA is neodecanoic acid, and THF is tetrahydrofuran). (B) Depiction of a directing-group simplifying the synthesis of a given compound. (C) Examples of monomers with directing groups (1 and 2) used in DArP with the polymerization conditions (CPME is cyclopentyl methyl ether). (D) Depiction of the π -complex formed in the catalytic cycle for DArP (see ref. 28). (E) Proposed effect of a directing group on the more frequent formation of the π -complex formed in the catalytic cycle for DArP.

conditions, and the outcomes (M_n, yield, and rr), illustrating that these conditions provide P3HET with a range of values for regioregulairty, yield, and M_n. Of these methods, DArP and Oxi-DArP offer the simplest pathway towards monomer and polymer synthesis. ^{14–17} However, a lingering issue with DArP and Oxi-DArP is the propensity for side-reactions to occur resulting in undesired couplings or defects. ^{18,19} In the case of P3HET, these defective couplings lead to increases in head to head (HH) or tail to tail (TT) couplings, reducing the overall rr of the polymer. For example, we

have previously reported conditions that provide P3HET-DArP (from 2-bromo-3-hexylesterthiophene) with an M_n of 11.7 kDa, in 55% yield, with a rr of 96%, and, comparatively, P3HET-Oxi-DArP affords P3HET in lower yield (44%), rr (86%), but with higher M_n (14.9 kDa), shown in Figure 1A. It is also clear from Figure 1A that P3HET-Stille and P3HET-SCTP provide P3HET with significantly improved rr (98% and >99%, respectively), yield (69%, and 79%, respectively), and M_n in the case of P3HET-SCTP (30.6 kDa). Although these methods provide the best polymerization outcomes for P3HET, the extended monomer synthesis makes them less appealing than DArP. Given the increasing appearance of ester-functionalized thiophene monomers, determining conditions for their polymerization via DArP with minimization of defects is imperative. To this end, a strategy that enables the synthesis of P3HET-DArP with improved M_n, yield, and rr compared to the previously reported conditions is to utilize the ester-moiety as a directing group for C-H activation.

A directing group is a lewis-base, such as an aza-heterocycle, ketone, ester, or amide, that can bind to the metal-center of the catalyst, increasing the frequency of interactions the catalyst has with the desired C-H bond.^{20–23} Directing-groups are often encountered in small-molecule C-H activation to facilitate site-selective activation of a desired C-H bond or to promote reactivity of a difficult to activate C-H bond (see Figure 1B).^{22,24} However, application of such a synthetic strategy to DArP remains limited.^{25,26} For example, we have reported the study of the diester-bithiophene,1, shown in Figure 1C, for the synthesis of perfectly alternating donor-acceptor copolymers. In contrast to the monomer used to synthesize P3HET-DArP (Figure 1A), the C-H bond designated for activation is adjacent to the ester moiety, as opposed to a bromine. This renders the ester as a directing group, specifically to enhance productive C-H activation during the polymerization. Indeed, we found this unit to be highly reactive for C-H activation (with the

conditions detailed in Figure 1C), requiring the careful selection of its aryl dibromide comonomer.²⁵ Here the ester-directing group likely did facilitate C-H activation of the desired monomer, but due to the close proximity of the ester moieties to the neighboring C-H bonds of the comonomer along the polymer backbone, e.g. bithiophene or bithiazole, the reactivity was difficult to control. This study showed that when an ester directing-group is incorporated into one of the monomers for a copolymerization, the possibility of activation of a C-H bond of the comonomer unit within the polymer backbone to form branched or cross-linked structures must be considered. As detailed in our previously reported study for monomer 1, the activation of β-protons or distal protons along the polymer backbone with the assistance of a neighboring directing group is dependent on the specific reactivity of the proton, such as its propensity to undergo C-H activation, and the conformation of the polymer backbone, e.g. coplanar or twisted.²⁵ From the findings of this study, the influence of the reactivity of a hydrogen along the backbone was ascribed to its acidity and the electronics of the ring to which it is attached. Additionally, a coplanar conformation is likely required in order for the directing group to place the metal catalyst near the site of C-H activation along the polymer backbone, and any twisting along the polymer backbone, which can occur through the steric interactions of neighboring substituents, can inhibit the activation of a C-H bond. When the same conditions used for the polymerization of the diester bithiophene (monomer 1) were applied for the preparation of amide functionalized polythiophenes (P3AAT) via homopolymerization, using monomers such as 2 (Figure 1C) where, again, the desired C-H bond to undergo activation is adjacent to the carbonyl directing-group, the rr obtained for the polymer product was nearly quantitative (>99%) and no branching was observed.²⁷ As with P3HET (Figure 1A), which has been prepared successfully using DArP with the exclusion of βdefects, the electronics of the thiophene ring for P3AAT and the steric hinderance of the

neighboring substituents likely inhibit the approach of the catalyst and subsequent activation of neighboring C-H bonds along the polymer backbone. From this study we suspected that the amide is functioning as a directing group to facilitate the site-selective C-H activation of the desired proton, allowing for the suppression of undesired couplings and the introduction of defects (HH or TT), providing high values for rr.

In addition to these experimental results, the mechanistic study performed by Fagnou and Gorelsky offers further insight.²⁸ As depicted in Figure 1D (Route A), with typical direct arylation (no directing group present) the critical interaction, which will lead to C-H activation, of the monomer to the palladium metal-center is dependent on the formation of the π -complex, INT-II. As described by Fagnou and Goreslky et al., the formation of INT-II is dependent on the availability of a vacant coordination site on the Pd^{II} metal-center, and the major energy barrier just before the C-H activation step is associated with the distortion of the Pd-complex to accommodate the approaching monomer (represented by the ester thiophene). This intermediate is the highest in energy and occurs just before the concerted metallation deprotonation (CMD) step. Given the high energy associated with this intermediate, its formation may be relatively limited or unfavorable under certain circumstances allowing for defect forming pathways to be more frequently undertaken leading to undesired couplings, such as the head to head (HH) defect depicted in Figure 1D. 14,29 In comparison, when the ester functionality is present adjacent to the site of C-H activation (Route B, Figure 1E), the ester can function as a ligand placing the desired site of C-H activation within good proximity to the Pd^{II} metal-center leading to more instances of π -complex formation and C-H activation. 20,22 This type of reactivity has been described for ester directing groups by Yu et al., where an ester can displace a weak ligand, such as a carboxylic acid present in DArP, allowing for the facile activation of otherwise difficult to access C-H bonds.³⁰ These findings

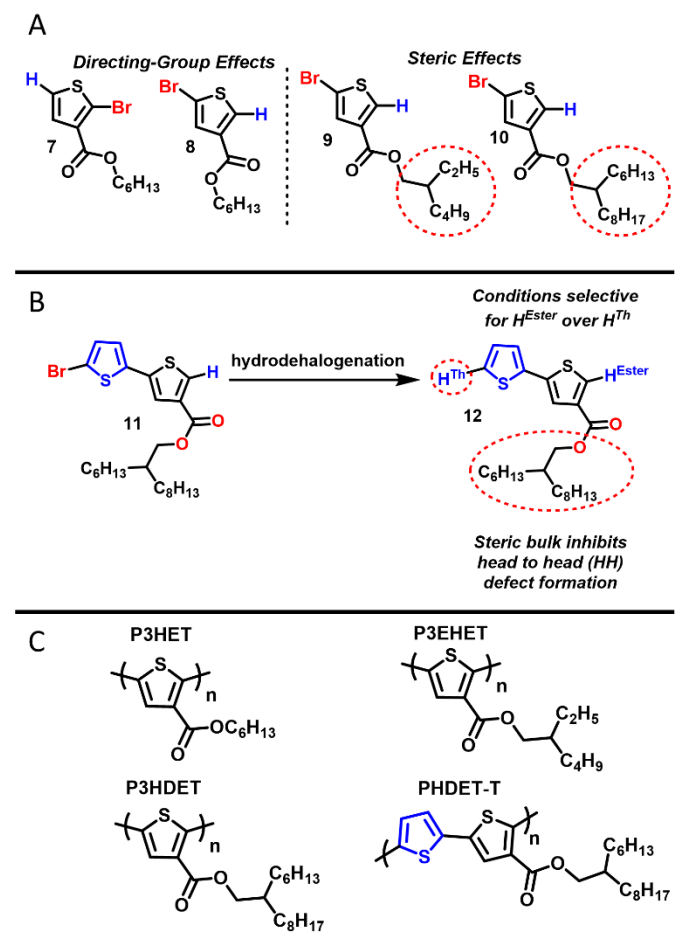


Figure 2. (A) Monomers used for studying the effect of a directing group (7 and 8) and the effect of sterics (9 and 10). (B) The rationally designed monomer, 11, and depiction of the C-H bond selectivity and steric bulk inhibiting TT and HH defect formation, respectively. (C) The polymers prepared in this study.

indicate that ester-directing groups could be exploited to allow for the site-selective C-H activation and the minimization of defects in DArP.

In this study, we explore the use of the ester directing group for DArP by examining how changes in the DArP conditions and monomer structure influence defect formation (Figure 2A). Specifically, we find that utilizing the ester directing group allows for the site-selective C-H activation of the desired proton, allowing for high levels of regionegularity to be obtained. To this

end, P3HET (Figure 2C) was prepared from monomer 8 with M_n up to 15.9 kDa, with high rr (up to >99%), and yield (up to 94%) in only 16 hours (compared to the 48 hours previously reported with monomer 7). 11 We find that Cs₂CO₃ as a base and ethereal solvents, such as THF or CPME, play a critical role in maintaining high levels of rr. To understand how sterics near the desired site of C-H activation influence the polymerization outcome, specifically defect formation, we applied the optimal conditions for P3HET towards the synthesis of poly(2-ethylhexylthiophene-3poly(2-ethylhexylthiophene-3-carboxylate-2,5-diyl) carboxylate-2,5-diyl) (P3EHET) and (P3HDET) using monomers 9 and 10, shown in Figure 2C, respectively. We found that the 2ethylhexyl-ester, 9, does not lead to a significant reduction in rr, with the polymer product obtained having a M_n of 16.3 kDa, a rr of 98%, and a yield of 70%. With 2-hexyldecyl ester, 10, although a reaction was observed no polymer precipitate was afforded indicating a diminished reactivity for this monomer. This is likely due to the excessive steric bulk, which may slow down the critical steps in the catalytic cycle that could be sensitive to sterics, such as C-H activation and reductive elimination. From end-group analysis using ¹H-NMR, we find that hydrodehalogenation is occurring as the predominant side-reaction for both P3HET and P3EHET. Correlating this finding with the observed defects, also determined using ¹H-NMR, we propose potential routes for defect formation due to hydrodehalogenation of the monomer and subsequent C-H activation of the newly formed C-H bond. Based on the findings of P3HET, P3EHET, and P3HDET, we designed monomer 11 to be more resistant to defect formation. This was accomplished by incorporating steric bulk near the site of C-H activation to inhibit HH couplings, but with a thiophene-spacer to alleviate steric hindrance that may inhibit polymer synthesis overall. Furthermore, the lower reactivity of the thiophene C-H bond (HTh, Figure 2B) relative to that of the ester-thiophene (H^{Ester}, Figure 2B) allows for the inhibition of TT defects consequential of hydrodehalogenation. The structural variation of this monomer is supported with the results of the polymerization where poly(2-Hexyldecyl [2,2'-bithiophene]-4-carboxylate -5,5'-diyl) (PHDET-T, Figure 2C), which is prepared with an M_n of 26 kDa, a rr of >99%, and in 73% yield. This study provides a simple, straightforward strategy for obtaining ester-functionalized thiophene polymers with high M_n and yield, by exploring the directing group ability of the ester and uses a comprehensive defect analysis to inspire the rational design of a monomer to promote regioselectivity.

Results and Discussion.

Synthesis of P3HET, P3EHET, and P3HDET.

Scheme 1. Study of the monomer structure and DArP conditions for the synthesis of P3HET, P3EHET, and P3HDET.

The complete details regarding monomer and polymer synthesis can be found in the supporting information (SI). The intial portion of this study is focused on the preparation of P3HET, where the conditions that provided the greatest value for M_n without sacrificing rr or yield were applied to the subsequent polymerizations of monomers 8-11. It should be noted that using the Pd(OAc)₂-DMA conditions previously reported for monomer 7 did not afford any polymer precipitate for monomer 8, indicating these conditions are not optimal for this monomer. As such, the conditions previously reported with an ethereal solvent (CPME) were explored (Figure 1C).^{25,27} As, depicted in Scheme 1 with the results listed in Table 1, it was first determined if the

polymerization conditions used for the amide-functionalized monomer 2 (Figure 1C), which provided >99% rr for

Table 1. DArP conditions used and the polymerization outcomes.

Entry	Monomer	Base	Solvent (M)	Time (hr)	Mn (kDa) a;Da	Yield a (%)	RR ^b (%)	HH- TT ^b (%)	TT- HT ^b (%)	HT- HH ^b (%)
1	7	Cs ₂ CO ₃	CPME (0.2)	16	11.2; 1.24	85	94	2	4	-
2	8	Cs ₂ CO ₃	CPME (0.2)	16	12.9; 1.57	94	>99	< 1	< 1	-
3	8	Cs ₂ CO ₃	CPME (0.2)	72	15.3; 1.52	87	98	1	1	-
4	8	K ₂ CO ₃	CPME (0.2)	16	12.5; 1.58	69	84	8	7	1
5	8	Cs ₂ CO ₃	THF (0.2)	16	13.6; 1.40	45	98	1	1	-
6	8	Cs ₂ CO ₃	Toluen e (0.2)	16	10.3; 1.60	65	94	3	3	-
7	8	Cs ₂ CO ₃	CPME (0.4)	16	15.9; 1.77	90	98	1	1	-
8	9	Cs ₂ CO ₃	CPME (0.4)	16	16.3; 1.41	70	98	1	1	-
9	10	Cs ₂ CO ₃	CPME (0.4)	16	NP	NP	-	-	-	-

^aMeasured after purification by Soxhlet Extraction. ^bDetermined using ¹H-NMR Spectroscopy at 500 MHz in CDCl₃ at 25°C.

the corresponding polymer, could have the same outcome for the ester thiophene monomer without a directing-group near the site of C-H activation (monomer 7 in Scheme 1). As shown with Entry 1 of Table 1, we found that P3HET was afforded with an M_n of 11.2 kDa, in 85% yield, but with

only 94% rr. Compared to the previously reported conditions for P3HET (see P3HET-DArP in Figure 1A), we observed an improvement in yield (85% versus 55%) and a reduction in polymerization time (16 versus 48 hours), but similar values for M_n (11.2 kDa versus 11.7 kDa) and rr (94% versus 96%) were obtained. Using the same conditions but just moving the site of C-H activation from the 2 to the 5-position of the thiophene ring, yielding monomer 8, we found an improvement in rr (>99%), yield (94%), and Mn (12.9), detailed with Entry 2 in Table 1. This improvement in rr matches what was observed with the polymerization of the amide functionalized monomer 2, and it is likely the inclusion of a directing group adjacent to the site of C-H activation which provides a near absolute value for rr by facilitating the site selective metallation of the monomer to the Pd-catalyst (see Figure 1E).

To probe how the modification of the conditions could influence the rr, yield, and M_n, we applied changes in the choice of base, solvent, and extended the polymerization time of monomer 8. By extending the reaction time to 72 hours (Entry 3 of Table 1), we find that the M_n improves (15.3 kDa) albeit with a minor decrease in rr (98%) and yield (87%). The 1% decrease in rr is likely due to the extended reaction time allowing for more instances of undesired couplings, such as HH or tail to tail (TT), to occur. In comparison to Entry 2, changing the base from Cs₂CO₃ to K₂CO₃ led to a significant decrease in yield (69%) and rr (84%), which is shown with Entry 4 of Table 1. Although K₂CO₃ provides acceptable polymerization outcomes for DArP-P3HET when Pd(OAc)₂ is used as the catalyst and DMA as the solvent, the conditions used here vary greatly from those. Studied extensively in numerous reports by Ozawa et al., Cs₂CO₃ is the optimal base for when ethereal solvents are employed, such as tetrahydrofuran (THF) or cyclopentyl methyl ether (CPME). To rationalize the lower yield and rr, it is likely that K₂CO₃ exhibits a lower reactivity for the given set of conditions, and so proton abstraction and metallation of the monomer

is likely occuring at a diminished rate. This would inturn potentially allow for increased instances of HH and TT defect formation, rather than the desired head to tail (HT) coupling. When the solvent is changed to THF from CPME (Entry 5 of Table 1), similar results to those of Entry 2 are obtained with regards to M_n (13.6 kDa) and rr (98%), but the yield decreases dramatically (45%). In contrast, toluene (Entry 6 of Table 1) provides a decreased M_n (10.3 kDa), yield (65%), and rr (94%). As described in various reports, toluene has been shown to facilitate defect formation leading to sacrifices in yield and M_n for a variety of DArP protocols.^{31,34} Increasing the concentration from 0.2 to 0.4 M (Entry 7 of Table 1), provided the highest M_n (15.9 kDa) with good yield (90%) and rr (98%). Compared to the previously reported DArP conditions for P3HET, which are described in Figure 1A, those detailed in Entry 7 provided a significant advancement.

Using the conditions detailed in Entry 7, which provided the highest M_n without significantly sacrificing yield or rr, we were interested to explore how steric influence near the site of C-H activation influences the outcome of the polymerization. For this we replaced the linear n-hexyl alkyl chain on the ester with a branched 2-ethylhexyl (monomer 9) and 2-hexyldecyl (monomer 10), shown in Figure 2A. With monomer 9, we were able to obtain polymer product (P3EHET) using the same conditions from Entry 7 with comparable values for M_n (16.3 kDa) and rr (98%), although with a diminished yield (70%), shown with Entry 8 of Table 1. With monomer 10, we were not able to obtain any polymer precipitate (P3HDET) from the reaction, indicating that the 2-hexyldecyl chains inhibit the polymerization by the steric bulk (Entry 9 of Table 1). Points of the polymerization where the steric bulk of the 2-hexyldecyl chains could inhibit growth of the polymer could be during the formation of intermediates or transition states near the CMD or reductive elimination steps. ^{35–42} As detailed in Figure S18A and S18B, the polymerization of monomer 10 may be stagnated due to steric congestion between 2-hexyldecyl substituents during

the approach of the monomer to the transition metal-complex (S1 and S5), during C-H activation or the CMD step (S2 and S7), or during reductive elimination (S3 and S8). These results demonstrate the potential limitations for this set of DArP conditions in handling steric bulk, and they provide insight into how to design monomers to mitigate the steric bulk, such as monomer 11 (Figure 2).

Defect Analysis of P3HET and P3EHET.

¹H-NMR defect analysis was performed for all of the entries in Table 1, with that for P3HET and P3EHET described below. Noonan and Pomerantz perfromed extensive NMR studies on P3HET allowing for the various defects to be quantified and the end-groups to be assigned. 13,43-47 The potential triads, either HT-HT, TT-HT, HH-TT, and HT-HH are shown in Figure 3C, along with a representative expanded view of the aromatic region for P3HET in Figure 3A and P3EHET in Figure 3B. End-groups with their expected values for chemical shifts are also provided in Figure 3C. Relative amounts for triads can be extracted from the aromatic region (8.20-7.55 ppm), allowing for the accurate determination of the identity and relative quantity of defects. While the alkyl region (4.16-4.08 ppm) can be used for measuring defect content, as it often is for P3HT for example, with P3HET the defect resonances here suffer from significant overlap even with the desired alkyl resonance (4.20 ppm), which is broad, making an accurate determination of the exact quantity of a specific defect-triad challenging. 11,48,49 Percentages for the three triads describing defects (TT-HT, HH-TT, and HT-HH) are provided in Table 1, and the ¹H-NMR spectra from which they are extracted are provided in the SI. For P3HET (Entries 1-7 of Table 1), it can be seen that triads containg TT defects, such as TT-HT (7.92 ppm) and HH-TT (7.60 ppm), form predominantly, indicating that TT defect formation is more favorable than HH. It is only with Entry 4, which used K₂CO₃ as the base and suffers from the lowest value for rr (84%), that the

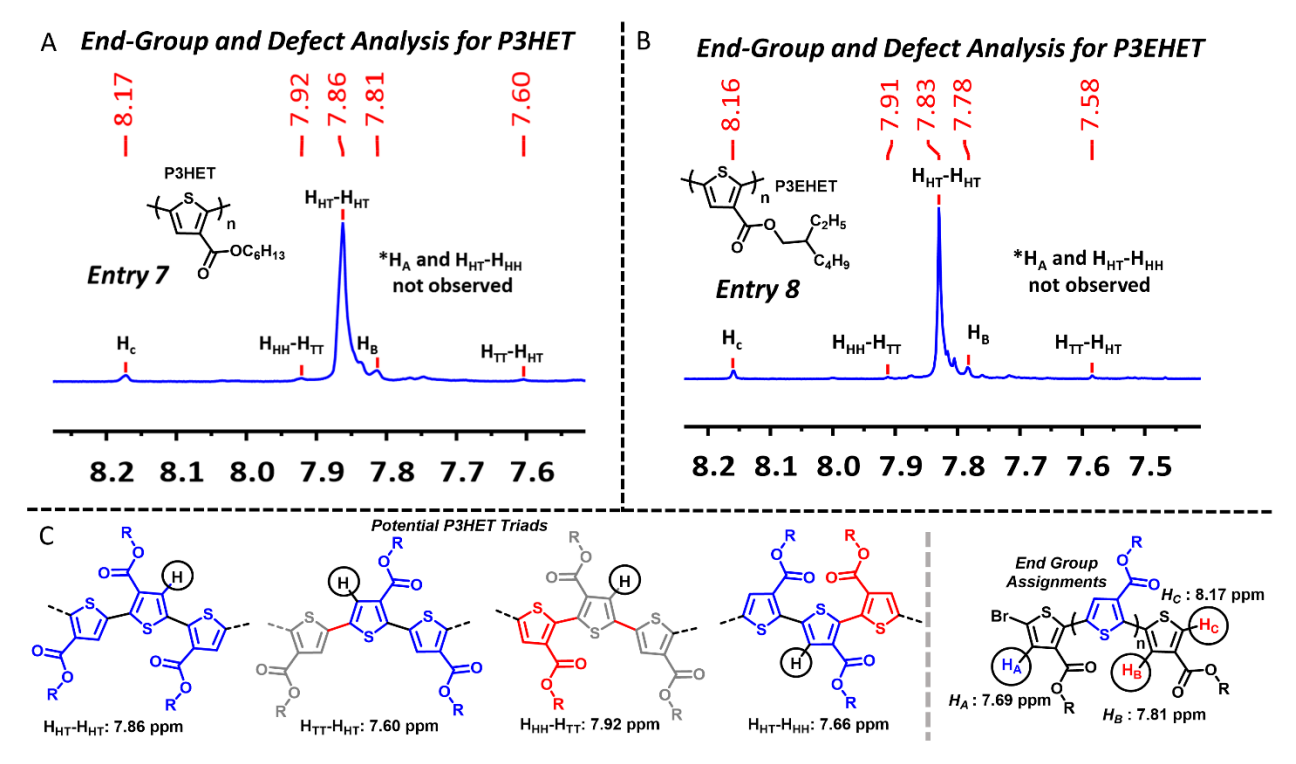


Figure 3. (A) An example (Entry 7 of Table 1) of the end-groups and defects observed for P3HET synthesized via DArP. (B) An example (Entry 8 of Table 1) of the end-groups and defects observed for P3EHET synthesized via DArP. (C) Depictions of the triads (HT-HT, TT-HT, HH-TT, and HT-HH) that can potentially form (right) and the potential end-groups (left).

HT-HH triad is observed (7.66 ppm, see Figure S11 in SI for spectrum). When the ester is employed as a directing group (Entries 2-7 of Table 1), it can be seen that the HH-TT and HT-HH defects occur in similar quantities, and it is only with Entry 1, which does not contain a directing group near the site of C-H activation, that TT-HT couplings occur in greater quantities (4%) than HH-TT (2%). When analyzing the ¹H-NMR for the end-groups present, only the protons adjacent to the ester directing group (8.17 and 7.81 ppm) are observed, shown in Figure 3C. The hydrogen corresponding to the halogenated end-group (7.69 ppm) is not observed for the entries provided, indicating that hydrodehalogenation is occuring. Hydrodehalogenation is prevalent throughout

DArP, which can inhibit high yields and M_n from being obtained, and its implication in defect formation is discussed further below.^{48,50–53}

For monomer 9, which yields P3EHET, the expected values for chemical shift of the end-groups and defects are expected to be similar to that of P3HET, and they are found to be shifted only slightly (~0.1-0.3 ppm upfield), which is shown in Figure 3B. As with P3HET, the observed defects correspond to the HH-TT (7.91 ppm) and TT-HT (7.58 ppm) triads. Additionally, the end-groups observed correspond to the protons adjacent to the ester directing group (8.16 and 7.78 ppm), while the halogenated end-group is not observed. The similarity in observed defects and end-groups for P3EHET and P3HET is expected, given that these structures only differ by an alkyl substituent, and that the additional steric interactions imposed by the 2-ethylhexyl subtiuent are not significant enough to inhibit or increase defect formation.

To provide some insight into the physical and electronic properties of the synthesized polymers, UV-vis absorption and GIXRD experiments of thin-films were conducted (see Figure S19 and Table S1). For P3HET it can be seen that there is very little change in the optical bandgap (E_g) with respect to rr, with the measured polymers all displaying a bandgap of approximately 2.19 eV. Additionally, the peak absorbance (λ_{max}) is approximately 480-490 nm for Entries 1, 2, 6, and 7, with no distinct correlation between rr and λ_{max} . As discolsed in a previous study, it is when the value for rr goes below 90% that significant changes arise in the physical and optical properties. From GIXRD experiments, the d_{100} was found to be very similar with values ranging from 19.6-19.8 Å, again showing no significant deviation due to changes in rr. For comparison, P3HET prepared via Stille polymerization or the previous conditions for DArP (see Figure 1A for the condtions used), shows similar values for λ_{max} and E_g at 485 and 479 nm and 2.17 and 2.18 eV, respectively. Additionally, the d_{100} -spacing for P3HET prepared using Stille polymerzation or

previous conditions for DArP (Figure 1A) are similar at 19.8 and 19.6 Å, respectively. For P3EHET (Entry 8 of Table 1), the thin-film measurment for UV-vis absorption and GIXRD experiments showed some deviation from P3HET. The optical bandgap was found to be 2.12 eV with a value for λ_{max} at 470 nm. From GIXRD experiments, it was found the inclusion of the branched 2-ethylhexyl substituent on P3EHET leads to an amporphous polymer, since no major peaks were observed in the diffraction pattern.

Potential Routes for Defect Formation.

The potential pathways for defect formation are outlined in Figure 4, which show defect formation for a monomer but the same reactions can be applied to a growing polymer chain. The derivation of these routes is based on observations from ¹H-NMR, where the end-groups present and quantity and types of defects observed are used for formulating the potential defect pathways. Of the end-groups observed for P3HET and P3EHET, none correspond to the halogenated end-group, indicating significant levels of hyrodehalogenation. Specifically, hydrodehalogenation (Figure 4A) may serve as a pathway for opening up different routes for the introduction of TT defects. In a study by Ozawa, it is proposed that hydrodehalogenation is occuring in a separate catalytic cycle that runs in parallel to the desired DArP reaction. ⁵⁰ Depicted in Figure 4A, the critical intermediates of Ozawa's mechanism for hydrodehalogenation are presented (13-18). Complex 13 (Figure 4A) is generated after oxidiative addition of the monomer and ligand

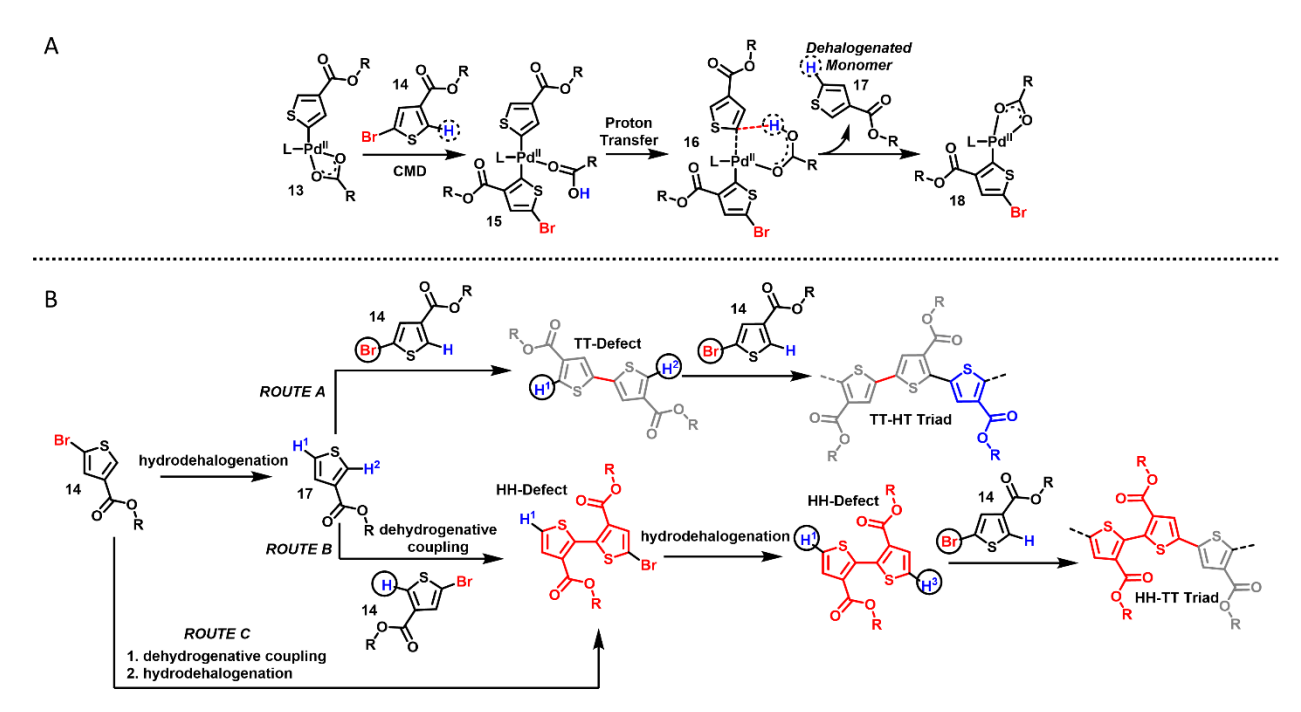


Figure 4. (A) Plausible mechanism for hydrodehalogenation (see ref. 41). (B) Examples of routes that can lead to the observed defects for P3HET, PEHET, and PHDET-T.

substitution of the bromine for a carboxylate. Then 15 is formed after C-H activation of another monomer, which regenerates the carboxylic acid from the carboxylate. The proton on the carboxylic acid then transfers from the acid to the other ester-thiophene to generate 16, which subsequently releases the dehalogenated monomer, 17. The dehalogenated monomer, 17, can then undergo a variety of coupling reactions to generate defective couplings within the polymer chain, which are depicted in Routes A-C of Figure 4B.

Three potential routes for defect formation are depicted in Figure 4B. For monomers 7-9, HH defects are likely introduced through dehydrogenative homocouplings, which may occur during generation of the active catalyst, reducing the Pd^{II} to Pd⁰. 11,14,29 TT defects, which have been previously described as occuring through C-Br/C-Br reductive couplings, can be generated after hydrodehalogenation followed by coupling with a halogenated monomer (shown in Figure 4B, Route A and Route B). While more are possible, the ones described here provide examples that

incorporate the results from the polymerization outcomes described in Table 1. Namely, that HH-TT and TT-HT are observed primarily and that halogenated end groups are not observed. The first, Route A, describes the generation of the TT-HT triad. This is shown as proceeding after the generation of dehalogenated monomer, 17, which undergoes a coupling with the monomer, 14, to yield a TT-defect. The subsequent coupling with another addition of monomer, 14, affords the TT-HT triad. In Route B, a dehydrogenative coupling affords a HH-defect. This can then undergo coupling with another addition of monomer to afford the HH-TT triad, or undergo hydrodehalogenation followed by coupling to afford the same triad. Route C is analogous to Route B, but the order of steps is switched so that hydrodehalogenation occurs after dehydrogenative coupling. In addition, while dehydrogenative couplings, i.e. C-H/C-H cross-couplings, can afford TT defects after hydrodehalgenation, such an occurrence is unlikely since this type of coupling more often proceeds with the assistance of a directing group and in the presence of a stoichiometric oxidant. 11,14 For a TT defect formation to be resultant of dehydrogenative coupling, H1 of compound 17 in Figure 4B would have to react, which is unfavorable relative to H² for the reasons just described.

Synthesis of PHDET-T.

From the analysis above regarding the observed defects in P3HET and P3EHET and their proposed pathways for formation, shown in Figure 4, monomer 11 was designed to be resistant to defect formation due to the influence of sterics and higher selectivity for the desired C-H bond, which is further discussed below. Shown in Figure 5A, the bulk of the 2-hexyldecyl substituent, while inhibiting polymer formation for monomer 4, should prevent HH couplings via dehydrogenative coupling (Entry 9 of

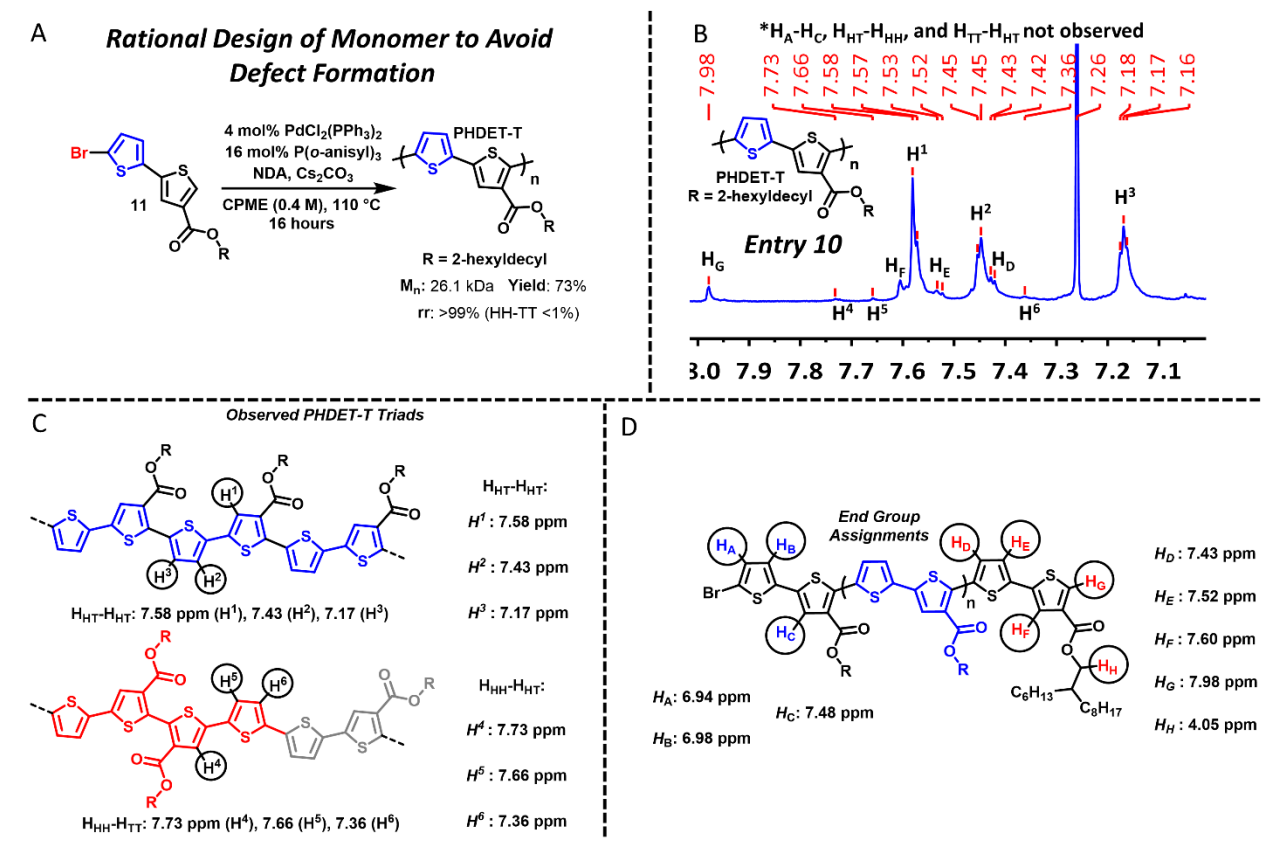


Figure 5. (A) Polymerization outcome for monomer 11 yielding PHDET-T. (B) ¹H-NMR for PHDET-T showing the aromatic region and the only observed defect-triad (HH-TT) and end (hydrodehalogenated). (C) Triads observed for PHDET-T. (D) End-group assignments for PHDET-T.

Table 1). In contrast to P3HDET, the presence of the thiophene spacer could alleviate the steric hindrance imposed by the bulky 2-hexyldecyl chains (see Figure S18C). This would allow for the formation of intermediates or transition states near the CMD or reductive elimination steps to be more energetically favorable, rather than hindered with steric bulk. Additionally, as described by Gorelsky et al., ester functionalized thiophenes are in a class considered the most reactive towards C-H activation, lowering the ΔG^{\ddagger} of the CMD step by approximately 2-3 kcal mol⁻¹ relative to the thiophene. Leclerc et al. have also reported that the energy of ΔG^{\ddagger} for the CMD step to be lower for protons near an electron-withdrawing substituent relative to unfunctionalized thiophene. S5,56

Such a preference in reactivity for the desired C-H bond could allow for a decrease and inhibition in the formation of defects. By applying the conditions used in Entry 7 of Table 1 towards the polymerization of monomer 11, we found that PHDET-T was prepared in good yield (73%), and with high values for Mn (26.1 kDa) and rr (> 99%), shown in Figure 5A. From these results we can conclude the thiophene serves as a spacer during the polymerization to mitigate the steric bulk brought upon by the 2-hexyldecyl alkyl chains, and that the reactivity of H^{Ester} towards C-H activation is greater than that of HTh (Figure 2B) leading to an increase in rr and M_n for the isolated polymer. Aside from regiorandom ester-thiophene polymers, attempts to prepare this polymer with high regioregularity have been limited. To our knowledge, only a dodecyl analog of this polymer has been previously prepared, but using Oxi-DArP, which afforded the polymer with diminished values for M_n (18.9 kDa) and rr (83%).⁵⁷ It is also worth noting that the directing group did not allow for activation of the β-protons on the thiophene unit, leading to insoluble material, which was a concern given our previous observations for this to occur during the copolymerization of monomer 1 (Figure 1B) with different comonomers.²⁵ This is likely due to an unfavorable conformation of the thiophene aryl group relative to the ester substituent or steric interactions inhibiting the approach of the palladium catalyst. Specifically, an unfavorable rotation or conformational change of the thiophene ring, relative to the aryl groups along the polymer backbone, may be required to place it in proximal location of the ester directing group allowing for C-H activation to occur.²⁵ Additionally, in the same fashion that bulky, branched carboxylates inhibit the activation of β -hydrogens for many conjugated polymers in DArP, the steric bulk of the 2-hexyldecyl substituent may impede the approach of the palladium catalyst to the protons along the backbone.⁴⁹ These findings demonstrate a simple, straightforward strategy for the preparation of donor-acceptor thiophene copolymers with high regioregularity and with good yields and M_n.

Defect analysis for PHDET-T was performed using ¹H-NMR, depicted in Figure 5B, and indicates that the observed resonances for the donor-acceptor polymer, PHDET-T, are shifted upfield (relateve to P3HET), which is expected given the inculsion of the more electron-rich thiophene. The HT-HT triad has shifted to 7.58 ppm, shown in Figure 5C, which is 0.28 ppm upfield form that of P3HET (7.86 ppm). Additionally, the protons correlating to the dehalogenated ester thiophene end-group shifted upfield by 0.19 ppm, such that H_G of PHEDET-T is 7.98 ppm (Figure 5) where H_C of P3HET is at 8.17 ppm (Figure 3B). Based on previous reports detailing the synthesis of simlar polymers and the observed change in chemical shift, the chemical shift of the proton adjacent to the ester for the other triads, TT-HT, HH-TT, and HT-HH, was expected to be approximately 7.32 ppm, 7.73 ppm, and 7.38 ppm, respectively (see Figure 5C and SI). 10,57 Of the triads pertaining to defects, only HH-TT is observed at 7.73 ppm, which is 0.19 ppm upfield from that of P3HET (see Figure 3B). As with P3HET and PEHET, the only end-groups observed for PHDET-T correspond to the protons adjacent to the ester directing group (depicted in Figure 5D). Assignments of the end-groups are provided in Figure S17 of the SI. This again illustrates the prevalance of hydrodehalogentation for this monomer, and that significant variation of the original monomer structure (monomer 8 relative to monomer 11) does not inhibit hydrodehalogenation entirely. The elimination of an observable level of the other triad, TT-HT, which was found with P3HET and P3EHET in equal amounts to HH-TT, indicates that this type of defect formation is inhibited via the strucutral modification provided with monomer 11 when compared to monomers 7-9. This again relates to the preferential reactivity for H^{Ester} over HTh to undergo C-H activation, which was described above, where the formation of a TT defect for monomer 11 would be generated in a pathway analogous to that for monomers 8 and 9, such as the one depicted in Route A of Figure 4B. However, since HTh is less reactive the defect-pathways, such as Route A, are

likely unfavorable in comparison to the desired HT coupling. The high regioregularity (>99%) for PHDET-T demonstrates how monomer design and DArP can be employed for the straightforward synthesis of highly regioregular donor-acceptor ester-thiophene polymers, which had previously only been afforded as regiorandom or with low regioregularity (rr of 83%).^{5,10,57} Overall, these results show that the structure of monomer 11 is highly resistant to defect formation, which is encouraging for applying these conditions and synthetic strategy more broadly toward the future synthesis of other ester-thiophene based donor-acceptor copolymers.

In order to analyze the physical and electronic properties of PHDET-T and provide a comparison to the regiorandom analogs, thin-film UV-vis and GIXRD experiments were performed. Compared to the polymers P3HET and P3EHET, PHDET-T showed a broader absorption (approximately 400-700 nm) with a red-shifted value for λ_{max} at 522 nm with an optical bandgap of 1.83 eV, consequential of the donor-acceptor polymer architure. Shouldering is also appearnt near approximately 600 nm, providing more distinguishing features to this polymers absroption profile. Additionally, the d_{100} spacing increased to 25.6 nm, which is due to the larger size of the 2-hexyldecyl substituent. In comparison, the regiorandom analogs of PHDET-T from a study by Zhang et al. show an approximately similar value for λ_{max} (near 520 nm), where the exact value is not provided, but from visual inspection the line shape of the abosrption profile for the regiorandom analog does not appear as broad or possess a distinct shoulder near 600 nm. ¹⁰ Additionally, the value for the bandgap is higher at 1.92 eV.

CONCLUSION

In conclusion, we present an extensive study of defect formation for ester functionalized thiophenes in DArP that shows how directing groups can be utilized to inhibit defect formation and promote the site-selective C-H activation of a desired proton. This allowed for P3HET to be prepared using DArP with M_n, yield, and rr similar to what is provided using more conventional

methods, such as Stille or SCTP. Based on the study of P3HET we then rationally designed a monomer that provides an ester-thiophene donor-acceptor polymer, PHDET-T, with high regioregularity (>99%), in good yield (73%), and with good M_n (26.2 kDa). Through extensive ¹H-NMR analysis we determine defect content for a variety of conditions and monomer structures, allowing us to reach a more defined conclusion about how the polymerization conditions and monomer structure lead to defect formation. Specifically, we find that dehydrohalogenation is the prominent pathway for the termination of polymer chains and the introduction of structural defects. To curtail this, the rationally designed monomer for PHDET-T uses electronics and sterics to resist defect formation. Specifically, differences in C-H bond reactivity avoids the potential TT defect formation brought upon by hydrodehaolgenation, and bulky alkyl substituents near the site of C-H activation limit HH defects formed through dehydrogenative coupling. Additionally, the facile route for monomer synthesis presented here and the findings regarding how the monomer structure, such as the inclusion of directing groups, can be easily tuned to allow for the inhibition of structural defects, will allow for the extension of this work to various conjugated polymers functionalized with a directing group.

ASSOCIATED CONTENT

Supporting Information. Monomer and polymer synthesis and characterization, including NMR, GIXRD, and UV-vis absorption.

AUTHOR INFORMATION

Corresponding Author

*barrycth@usc.edu.

ACKNOWLEDGMENT

This work was supported by the National Science Foundation (MSN under award number CHE-1904650 and CHE-1608891). We thank Professor Megan E. Fieser for assistance with GPC measurements.

REFERENCES

- (1) Moia, D.; Giovannitti, A.; Szumska, A. A.; Maria, I. P.; Rezasoltani, E.; Sachs, M.; Schnurr, M.; Barnes, P. R. F.; McCulloch, I.; Nelson, J. Design and Evaluation of Conjugated Polymers with Polar Side Chains as Electrode Materials for Electrochemical Energy Storage in Aqueous Electrolytes. *Energy Environ. Sci.* 2019. https://doi.org/10.1039/C8EE03518K.
- (2) Thompson, B. C.; Frechet, J. M. J. Polymer-Fullerene Composite Solar Cells. *Angew. Chem., Int. Ed.* **2008**, *47*, 58–77. https://doi.org/10.1002/anie.200702506.
- (3) Beaujuge, P. M.; Reynolds, J. R. Color Control in π-Conjugated Organic Polymers for Use in Electrochromic Devices. *Chem. Rev.* **2010**, *110* (1), 268–320. https://doi.org/10.1021/cr900129a.
- (4) Lei, T.; Guan, M.; Liu, J.; Lin, H.-C.; Pfattner, R.; Shaw, L.; McGuire, A. F.; Huang, T.-C.; Shao, L.; Cheng, K.-T.; Tok, J. B.-H.; Bao, Zhenan. Biocompatible and Totally Disintegrable Semiconducting Polymer for Ultrathin and Ultralightweight Transient Electronics. *Proc. Natl. Acad. Sci. U. S. A.* **2017**, *114* (Copyright (C) 2017 American Chemical Society (ACS). All Rights Reserved.), 5107–5112. https://doi.org/10.1073/pnas.1701478114.
- (5) Murphy, A. R.; Liu, J.; Luscombe, C.; Kavulak, D.; Fréchet, J. M. J.; Kline, R. J.; McGehee, M. D. Synthesis, Characterization, and Field-Effect Transistor Performance of Carboxylate-Functionalized Polythiophenes with Increased Air Stability. *Chem. Mater.* 2005, 17 (20), 4892–4899. https://doi.org/10.1021/cm050911d.
- (6) Noh, S.; Gobalasingham, N. S.; Thompson, B. C. Facile Enhancement of Open-Circuit Voltage in P3HT Analogues via Incorporation of Hexyl Thiophene-3-Carboxylate. *Macromolecules* **2016**, *49* (18), 6835–6845. https://doi.org/10.1021/acs.macromol.6b01178.
- (7) Liu, J.; Kadnikova, E. N.; Liu, Y.; McGehee, M. D.; Fréchet, J. M. J. Polythiophene Containing Thermally Removable Solubilizing Groups Enhances the Interface and the Performance of Polymer–Titania Hybrid Solar Cells. *J. Am. Chem. Soc.* **2004**, *126* (31), 9486–9487. https://doi.org/10.1021/ja047452m.
- (8) Chen, J.; Liao, Q.; Wang, G.; Yan, Z.; Wang, H.; Wang, Y.; Zhang, X.; Tang, Y.; Facchetti, A.; Marks, T. J.; Guo, X. Enhancing Polymer Photovoltaic Performance via Optimized Intramolecular Ester-Based Noncovalent Sulfur···Oxygen Interactions. *Macromolecules* **2018**, *51* (10), 3874–3885. https://doi.org/10.1021/acs.macromol.8b00161.

- (9) Zhang, M.; Guo, X.; Ma, W.; Ade, H.; Hou, J. A Polythiophene Derivative with Superior Properties for Practical Application in Polymer Solar Cells. *Adv. Mater.* **2014**, *26* (33), 5880–5885. https://doi.org/10.1002/adma.201401494.
- (10) Zhang, M.; Guo, X.; Yang, Y.; Zhang, J.; Zhang, Z.-G.; Li, Y. Downwards Tuning the HOMO Level of Polythiophene by Carboxylate Substitution for High Open-Circuit-Voltage Polymer Solar Cells. *Polym. Chem.* 2011, 2 (12), 2900–2906. https://doi.org/10.1039/C1PY00327E.
- (11) Gobalasingham, N. S.; Noh, S.; Thompson, B. C. Palladium-Catalyzed Oxidative Direct Arylation Polymerization (Oxi-DArP) of an Ester-Functionalized Thiophene. *Polym. Chem.* **2016**, *7* (8), 1623–1631. https://doi.org/10.1039/C5PY01973G.
- (12) Gobalasingham, N. S.; Pankow, R. M.; Thompson, B. C. Synthesis of Random Poly(Hexyl Thiophene-3-Carboxylate) Copolymers via Oxidative Direct Arylation Polymerization (Oxi-DArP). *Polym. Chem.* **2017**, 8 (12), 1963–1971. https://doi.org/10.1039/C7PY00181A.
- (13) Qiu, Y.; Worch, J. C.; Fortney, A.; Gayathri, C.; Gil, R. R.; Noonan, K. J. T. Nickel-Catalyzed Suzuki Polycondensation for Controlled Synthesis of Ester-Functionalized Conjugated Polymers. *Macromolecules* **2016**, *49* (13), 4757–4762. https://doi.org/10.1021/acs.macromol.6b01006.
- (14) Gobalasingham, N. S.; Thompson, B. C. Direct Arylation Polymerization: A Guide to Optimal Conditions for Effective Conjugated Polymers. *Progress in Polymer Science* **2018**, 83, 135–201. https://doi.org/10.1016/j.progpolymsci.2018.06.002.
- (15) Blaskovits, J. T.; Leclerc, M. C□H Activation as a Shortcut to Conjugated Polymer Synthesis. *Macromolecular Rapid Communications* **2018**, *θ* (0), 1800512. https://doi.org/10.1002/marc.201800512.
- (16) Okamoto, K.; Zhang, J.; Housekeeper, J. B.; Marder, S. R.; Luscombe, C. K. C–H Arylation Reaction: Atom Efficient and Greener Syntheses of π-Conjugated Small Molecules and Macromolecules for Organic Electronic Materials. *Macromolecules* 2013, 46 (20), 8059– 8078. https://doi.org/10.1021/ma401190r.
- (17) Bohra, H.; Wang, Mingfeng. Direct C-H Arylation: A "Greener" Approach towards Facile Synthesis of Organic Semiconducting Molecules and Polymers. *J. Mater. Chem. A* **2017**, No. Copyright (C) 2017 American Chemical Society (ACS). All Rights Reserved., Ahead of Print. https://doi.org/10.1039/c7ta00617a.
- (18) Broll, S.; Nübling, F.; Luzio, A.; Lentzas, D.; Komber, H.; Caironi, M.; Sommer, M. Defect Analysis of High Electron Mobility Diketopyrrolopyrrole Copolymers Made by Direct Arylation Polycondensation. *Macromolecules* **2015**, *48* (20), 7481–7488. https://doi.org/10.1021/acs.macromol.5b01843.
- (19) Kohn, P.; Huettner, S.; Komber, H.; Senkovskyy, V.; Tkachov, R.; Kiriy, A.; Friend, R. H.; Steiner, U.; Huck, W. T. S.; Sommer, J.-U.; Sommer, M. On the Role of Single Regiodefects and Polydispersity in Regioregular Poly(3-Hexylthiophene): Defect Distribution, Synthesis of Defect-Free Chains, and a Simple Model for the Determination of Crystallinity. *J. Am. Chem. Soc.* **2012**, *134* (10), 4790–4805. https://doi.org/10.1021/ja210871j.
- (20) Murai, S.; Kakiuchi, F.; Sekine, S.; Tanaka, Y.; Kamatani, A.; Sonoda, M.; Chatani, N. Efficient Catalytic Addition of Aromatic Carbon-Hydrogen Bonds to Olefins. *Nature* **1993**, *366* (6455), 529–531. https://doi.org/10.1038/366529a0.

- (21) Desai, L. V.; Stowers, K. J.; Sanford, M. S. Insights into Directing Group Ability in Palladium-Catalyzed C-H Bond Functionalization. *J. Am. Chem. Soc.* **2008**, *130* (40), 13285–13293. https://doi.org/10.1021/ja8045519.
- (22) Sambiagio, C.; Schönbauer, D.; Blieck, R.; Dao-Huy, T.; Pototschnig, G.; Schaaf, P.; Wiesinger, T.; Zia, M. F.; Wencel-Delord, J.; Besset, T.; Maes, B. U. W.; Schnürch, M. A Comprehensive Overview of Directing Groups Applied in Metal-Catalysed C–H Functionalisation Chemistry. *Chem. Soc. Rev.* **2018**. https://doi.org/10.1039/C8CS00201K.
- (23) Tomberg, A.; Muratore, M. É.; Johansson, M. J.; Terstiege, I.; Sköld, C.; Norrby, P.-O. Relative Strength of Common Directing Groups in Palladium-Catalyzed Aromatic C–H Activation. *iScience* **2019**, *20*, 373–391. https://doi.org/10.1016/j.isci.2019.09.035.
- Zhang, F.; Spring, D. R. Arene C-H Functionalisation Using a Removable/Modifiable or a Traceless Directing Group Strategy. *Chem. Soc. Rev.* **2014**, *43* (20), 6906–6919. https://doi.org/10.1039/C4CS00137K.
- (25) Pankow, R. M.; Ye, L.; Thompson, B. C. Influence of an Ester Directing-Group on Defect Formation in the Synthesis of Conjugated Polymers via Direct Arylation Polymerization (DArP) Using Sustainable Solvents. *Polym. Chem.* **2019**. https://doi.org/10.1039/C9PY00815B.
- (26) Kanbara, T.; Kuwabara, J.; Lu, W. Ru-Catalyzed Site-Selective Direct Arylation Polycondensation via Ortho -Metalation of Pyrrole Derivative. *IOP Conf. Ser.: Mater. Sci. Eng.* **2014**, *54*. https://doi.org/10.1088/1757-899X/54/1/012012.
- (27) Ye, L.; Pankow, R. M.; Horikawa, M.; Melenbrink, E. L.; Liu, K.; Thompson, B. C. Green Solvent Processed Amide-Functionalized Conjugated Poly-Mers Prepared via Direct Arylation Polymerization (DArP). *Macromolecules* **2019**. https://doi.org/10.1021/acs.macromol.9b02014.
- (28) Gorelsky, S. I.; Lapointe, D.; Fagnou, K. Analysis of the Palladium-Catalyzed (Aromatic)C–H Bond Metalation–Deprotonation Mechanism Spanning the Entire Spectrum of Arenes. *J. Org. Chem.* **2012**, *77* (1), 658–668. https://doi.org/10.1021/jo202342q.
- (29) Rudenko, A. E.; Thompson, B. C. Optimization of Direct Arylation Polymerization (DArP) through the Identification and Control of Defects in Polymer Structure. *J. Polym. Sci. A Polym. Chem.* **2015**, *53* (2), 135–147. https://doi.org/10.1002/pola.27279.
- (30) Li, G.; Wan, L.; Zhang, G.; Leow, D.; Spangler, J.; Yu, J.-Q. Pd(II)-Catalyzed C–H Functionalizations Directed by Distal Weakly Coordinating Functional Groups. *J. Am. Chem. Soc.* **2015**, *137* (13), 4391–4397. https://doi.org/10.1021/ja5126897.
- (31) Wakioka, M.; Kitano, Y.; Ozawa, F. A Highly Efficient Catalytic System for Polycondensation of 2,7-Dibromo-9,9-Dioctylfluorene and 1,2,4,5-Tetrafluorobenzene via Direct Arylation. *Macromolecules* **2013**, *46* (2), 370–374. https://doi.org/10.1021/ma302558z.
- (32) Wang, Q.; Takita, R.; Kikuzaki, Y.; Ozawa, F. Palladium-Catalyzed Dehydrohalogenative Polycondensation of 2-Bromo-3-Hexylthiophene: An Efficient Approach to Head-to-Tail Poly(3-Hexylthiophene). *J. Am. Chem. Soc.* **2010**, *132* (33), 11420–11421. https://doi.org/10.1021/ja105767z.
- (33) Wang, Q.; Wakioka, M.; Ozawa, F. Synthesis of End-Capped Regioregular Poly(3-Hexylthiophene)s via Direct Arylation. *Macromol. Rapid Commun.* **2012**, *33* (14), 1203–1207. https://doi.org/10.1002/marc.201200076.

- (34) Matsidik, R.; Komber, H.; Sommer, M. Rational Use of Aromatic Solvents for Direct Arylation Polycondensation: C–H Reactivity versus Solvent Quality. *ACS Macro Lett.* **2015**, *4* (12), 1346–1350. https://doi.org/10.1021/acsmacrolett.5b00783.
- (35) Tolentino, D. R.; Neale, S. E.; Isaac, C. J.; Macgregor, S. A.; Whittlesey, M. K.; Jazzar, R.; Bertrand, G. Reductive Elimination at Carbon under Steric Control. *J. Am. Chem. Soc.* **2019**, *141* (25), 9823–9826. https://doi.org/10.1021/jacs.9b04957.
- (36) Hartwig, J. Organotransition Metal Chemistry From Bonding to Catalysis, 1st ed.; University Science Books: Mill Valley, 2010.
- (37) Labinger, J. A. Tutorial on Oxidative Addition. *Organometallics* **2015**, *34* (20), 4784–4795. https://doi.org/10.1021/acs.organomet.5b00565.
- (38) Casado, A. L.; Espinet, P. On the Configuration Resulting from Oxidative Addition of RX to Pd(PPh3)4 and the Mechanism of the Cis-to-Trans Isomerization of [PdRX(PPh3)2] Complexes (R = Aryl, X = Halide). *Organometallics* **1998**, *17* (5), 954–959. https://doi.org/10.1021/om9709502.
- (39) Hartwig, J. F. Carbon–Heteroatom Bond-Forming Reductive Eliminations of Amines, Ethers, and Sulfides. *Acc. Chem. Res.* **1998**, *31* (12), 852–860. https://doi.org/10.1021/ar970282g.
- (40) Pérez-Temprano, M. H.; Gallego, A. M.; Casares, J. A.; Espinet, P. Stille Coupling of Alkynyl Stannane and Aryl Iodide, a Many-Pathways Reaction: The Importance of Isomerization. *Organometallics* **2011**, *30* (3), 611–617. https://doi.org/10.1021/om100978w.
- (41) Cordovilla, C.; Bartolomé, C.; Martínez-Ilarduya, J. M.; Espinet, P. The Stille Reaction, 38 Years Later. *ACS Catal.* **2015**, *5* (5), 3040–3053. https://doi.org/10.1021/acscatal.5b00448.
- (42) Xue, L.; Lin, Z. Theoretical Aspects of Palladium-Catalysed Carbon-Carbon Cross-Coupling Reactions. *Chem. Soc. Rev.* **2010**, *39* (5), 1692–1705. https://doi.org/10.1039/B814973A.
- (43) Pomerantz, M.; Cheng, Y. Ester Substituted Bithiophenes. Abnormally Low Dihedral Angle and Rotation Barrier Due to Dipolar Stabilization. *Tetrahedron Lett.* **1999**, *40* (17), 3317–3320. https://doi.org/10.1016/S0040-4039(99)00500-6.
- (44) Pomerantz, M.; Amarasekara, A. S.; Dias, H. V. R. Synthesis and Solid-State Structures of Dimethyl 2,2'-Bithiophenedicarboxylates. *J. Org. Chem.* **2002**, *67* (20), 6931–6937. https://doi.org/10.1021/jo020307b.
- (45) Pomerantz, M.; Cheng, Y.; Kasim, R. K.; Elsenbaumer, R. L. Poly(Alkyl Thiophene-3-Carboxylates). Synthesis, Properties and Electroluminescence Studies of a Polythiophene with a Carbonyl Group Attached to the Ring. *Synth. Met.* **1997**, *85* (1–3), 1235–1236. https://doi.org/10.1016/S0379-6779(97)80218-4.
- (46) Pomerantz, M.; Yang, H.; Cheng, Y. Poly(Alkyl Thiophene-3-Carboxylates). Synthesis and Characterization of Polythiophenes with a Carbonyl Group Directly Attached to the Ring. *Macromolecules* **1995**, *28* (17), 5706–5708. https://doi.org/10.1021/ma00121a003.
- (47) Pomerantz, M.; Cheng, Y.; K. Kasim, R.; L. Elsenbaumer, R. Poly(Alkyl Thiophene-3-Carboxylates). Synthesis, Properties and Electroluminescence Studies of Polythiophenes Containing a Carbonyl Group Directly Attached to the Ring. *J. Mater. Chem.* **1999**, *9* (9), 2155–2163. https://doi.org/10.1039/A902504I.
- (48) Pouliot, J.-R.; Wakioka, M.; Ozawa, F.; Li, Y.; Leclerc, M. Structural Analysis of Poly(3-hexylthiophene) Prepared via Direct Heteroarylation Polymerization. *Macromol. Chem. Phys.* **2016**, *217* (13), 1493–1500. https://doi.org/10.1002/macp.201600050.

- (49) Rudenko, A. E.; Thompson, B. C. Influence of the Carboxylic Acid Additive Structure on the Properties of Poly(3-Hexylthiophene) Prepared via Direct Arylation Polymerization (DArP). *Macromolecules* **2015**, *48* (3), 569–575. https://doi.org/10.1021/ma502131k.
- (50) Iizuka, E.; Wakioka, M.; Ozawa, F. Mixed-Ligand Approach to Palladium-Catalyzed Direct Arylation Polymerization: Synthesis of Donor–Acceptor Polymers with Dithienosilole (DTS) and Thienopyrroledione (TPD) Units. *Macromolecules* **2015**, *48* (9), 2989–2993. https://doi.org/10.1021/acs.macromol.5b00526.
- (51) Parisien, M.; Valette, D.; Fagnou, K. Direct Arylation Reactions Catalyzed by Pd(OH)2/C: Evidence for a Soluble Palladium Catalyst. *J. Org. Chem.* **2005**, 70 (19), 7578–7584. https://doi.org/10.1021/jo051039v.
- (52) Dou, J.; Chen, Z.; Ma, C. Regioregularity and Properties of the Poly(3-Hexylthiophene) Synthesized by Palladium Catalyzed Direct CH Arylation Polycondensation under Different Reaction Conditions. *Synth. Met.* **2014**, *196*, 117–124. https://doi.org/10.1016/j.synthmet.2014.07.022.
- (53) Ahmadi, Z.; McIndoe, J. S. A Mechanistic Investigation of Hydrodehalogenation Using ESI-MS. *Chem. Commun.* **2013**, 49 (98), 11488–11490. https://doi.org/10.1039/C3CC46271D.
- (54) Gorelsky, S. I. Origins of Regioselectivity of the Palladium-Catalyzed (Aromatic)CH Bond Metalation–Deprotonation. *Coord. Chem. Rev.* **2013**, *257* (1), 153–164. https://doi.org/10.1016/j.ccr.2012.06.016.
- (55) Blaskovits, J. T.; Johnson, P. A.; Leclerc, M. Mechanistic Origin of β-Defect Formation in Thiophene-Based Polymers Prepared by Direct (Hetero)Arylation. *Macromolecules* **2018**. https://doi.org/10.1021/acs.macromol.8b01142.
- (56) Morin, P.-O.; Bura, T.; Sun, B.; Gorelsky, S. I.; Li, Y.; Leclerc, M. Conjugated Polymers à La Carte from Time-Controlled Direct (Hetero)Arylation Polymerization. *ACS Macro Lett.* **2015**, *4* (1), 21–24. https://doi.org/10.1021/mz500656g.
- (57) Zhang, Q.; Chang, M.; Lu, Y.; Sun, Y.; Li, C.; Yang, X.; Zhang, M.; Chen, Y. A Direct C– H Coupling Method for Preparing π-Conjugated Functional Polymers with High Regioregularity. *Macromolecules* **2018**. https://doi.org/10.1021/acs.macromol.7b02390.